

## Growth of silicon on tungsten diselenide

Qirong Yao, Rik van Bremen, and Harold J. W. Zandvliet

Citation: *Appl. Phys. Lett.* **109**, 243105 (2016); doi: 10.1063/1.4972036

View online: <http://dx.doi.org/10.1063/1.4972036>

View Table of Contents: <http://aip.scitation.org/toc/apl/109/24>

Published by the [American Institute of Physics](#)

---

### Articles you may be interested in

[Pressure and temperature-dependent Raman spectra of MoS<sub>2</sub> film](#)

*Appl. Phys. Lett.* **109**, 242101242101 (2016); 10.1063/1.4968534

[Correlation of nanostructure changes with the electrical properties of molybdenum disulfide \(MoS<sub>2</sub>\) as affected by sulfurization temperature](#)

*Appl. Phys. Lett.* **109**, 242104242104 (2016); 10.1063/1.4971386

[Local conductance mapping of water-intercalated graphene on mica](#)

*Appl. Phys. Lett.* **109**, 241602241602 (2016); 10.1063/1.4972233

[Edge plasmons in monolayer black phosphorus](#)

*Appl. Phys. Lett.* **109**, 241902241902 (2016); 10.1063/1.4972109

[Germanium-on-silicon nitride waveguides for mid-infrared integrated photonics](#)

*Appl. Phys. Lett.* **109**, 241101241101 (2016); 10.1063/1.4972183

[Gamma bandgap determination in pseudomorphic GeSn layers grown on Ge with up to 15% Sn content](#)

*Appl. Phys. Lett.* **109**, 242107242107 (2016); 10.1063/1.4971397

---

Get the scoop on  
science funding & policy

Free sign-up  
for FYI emails

AIP American Institute of Physics



## Growth of silicon on tungsten diselenide

Qirong Yao,<sup>a)</sup> Rik van Bremen,<sup>a),b)</sup> and Harold J. W. Zandvliet

*Physics of Interfaces and Nanomaterials, MESA+ Institute for Nanotechnology, University of Twente, P.O. Box 217, 7500 AE Enschede, The Netherlands*

(Received 29 August 2016; accepted 29 November 2016; published online 16 December 2016)

Here, we report a scanning tunneling microscopy and spectroscopy study of the growth of silicon on a tungsten diselenide ( $\text{WSe}_2$ ) substrate. We have found convincing experimental evidence that silicon does not remain on the  $\text{WSe}_2$  substrate but rather intercalates between the top layers of  $\text{WSe}_2$ . Upon silicon deposition, the flat  $\text{WSe}_2$  surface converts into a surface with a hill-and-valley structure. The lattice constant of the hill-and-valley structure is identical to the lattice constant of  $\text{WSe}_2$  and the transition from hills to valleys is very gradual, suggesting that the top layer is composed of pristine  $\text{WSe}_2$ . In order to verify this conjecture, we have removed the height information from our scanning tunneling microscopy signal and obtained chemical contrast of the surface by recording  $dI/dz$ , rather than the conventional regulation voltage of the  $z$ -piezo. The spatially resolved  $dI/dz$  maps provide compelling evidence that the deposited silicon does indeed not reside on top of the  $\text{WSe}_2$  substrate. *Published by AIP Publishing.*

[<http://dx.doi.org/10.1063/1.4972036>]

Since the isolation of graphene by Novoselov and Geim,<sup>1</sup> two-dimensional (2D) materials have received a lot of attention. The method of delaminating graphite down to a single layer is facilitated by the crystal structure of graphite, which consists of 2D layers that are weakly bonded to each other via van der Waals forces.<sup>2</sup> Besides graphite, other 2D materials such as the transition metal dichalcogenides (TMDs) also consist of these weakly van der Waals bonded layers. The chemical composition of each of these TMDs is  $\text{MX}_2$ , where M refers to a transition metal, e.g., molybdenum or tungsten, and X stands for a chalcogen such as sulfur or selenium. Each TMD layer consists of three sheets with hexagonal symmetry that are covalently bonded to each other. In each of these triple layers, one layer of transition metal atoms is sandwiched in between two layers of chalcogen atoms. Since the TMDs have a similar layered structure as graphite, it is not surprising that a renewed interest in the TMDs aroused when it was found possible to also exfoliate these materials to a single layer.<sup>3</sup> As such, it was found that the physical properties of TMDs such as the band gap<sup>4</sup> and electron-phonon coupling<sup>5</sup> depend on the number of TMD triple layers.

Pristine and free-standing graphene is gapless, and therefore this material cannot be used as the key material for the field-effect based devices. Many scientists have, however, tried to open a band gap in pristine graphene by breaking the sub-lattice symmetry.<sup>6,7</sup> So far, these attempts have failed or resulted in a strong degradation of the charge carrier mobilities. A more suitable 2D material for realizing a field-effect transistor is silicene, the silicon analogue of graphene, which naturally already displays a broken sub-lattice symmetry. The charge carriers in silicene have been predicted to behave similar to the massless Dirac fermions of graphene.<sup>8</sup> Unlike graphite and the TMDs, silicene does not occur in

nature and therefore it has to be synthesized. Several research groups have shown that silicene can be grown on  $\text{Ag}(111)$ .<sup>9-12</sup> Silicene synthesized on  $\text{Ag}(111)$  even displays a linear dispersion relation;<sup>11</sup> however, the exact origin of this linear energy band is still under debate.<sup>13</sup> Unfortunately, silicene has a strong electronic coupling with the  $\text{Ag}(111)$  substrate and as a result loses its Dirac fermion characteristics.<sup>14</sup> To protect the unique electronic properties of silicene, the electronic coupling with the substrate should be reduced as much as possible. TMDs like  $\text{WSe}_2$  and  $\text{MoS}_2$ , which have no dangling bonds, are atomically flat over large areas, and have a band gap, seem to fit all the requirements to support the growth of silicene as the interaction with the 2D adlayer is only via very weak van der Waals forces.<sup>15</sup> This weak interaction will help to preserve the important electronic properties near the Fermi level. The growth of silicon on  $\text{MoS}_2$  has already been studied.<sup>16,17</sup> Another appealing two-dimensional material is germanene.<sup>18-21</sup> Recently, the synthesis of germanene on  $\text{MoS}_2$  has been reported.<sup>22</sup> The density of states of germanene on  $\text{MoS}_2$  exhibits a well-defined V-shape, which is one of the hallmarks of a two-dimensional Dirac material.<sup>23</sup>

In this article, we report on the growth of sub-monolayers of silicon on tungsten diselenide ( $\text{WSe}_2$ ). Upon deposition of silicon, the atomically flat  $\text{WSe}_2$  surface converts into a surface with a hill-and-valley structure. Guided by our high-resolution scanning tunneling microscopy (STM) and spectroscopy (STS) measurements, we provide compelling evidence that silicon does not grow on top of  $\text{WSe}_2$  but intercalates between the  $\text{WSe}_2$  layers.

The experiments were carried out in a system equipped with a room temperature Omicron STM (STM-1). The base pressure in the system is below  $3 \times 10^{-11}$  mbar. All the STM and STS measurements were conducted at room temperature. The synthetic  $\text{WSe}_2$  samples purchased from HQ Graphene were cleaned by mechanical exfoliation in ambient conditions after which they were immediately mounted on a sample

<sup>a)</sup>Q. Yao and R. van Bremen contributed equally to this work.

<sup>b)</sup>Author to whom correspondence should be addressed. Electronic mail: r.vanbremen@utwente.nl

holder and inserted into the ultra-high vacuum system. Limited contamination is expected because the samples are non-reactive. Silicon was deposited on the WSe<sub>2</sub> samples via the resistive heating of a small piece of a silicon wafer. In order to calibrate the silicon source, we deposited a fraction of a monolayer of silicon on a Ge(001) substrate at room temperature. Subsequently, the Ge(001) substrate was mildly annealed at a temperature 450–500 K. After that, we determined the coverage of the epitaxial silicon islands.

Before the deposition of silicon, the samples of freshly cleaved WSe<sub>2</sub> are characterized by the constant current topography STM images. In this STM mode, the tip-sample distance is adjusted as to keep a constant tunneling current while the extension of the z-piezo is recorded. The lattice constant of the hexagonal lattice of WSe<sub>2</sub> is 3.28 Å.<sup>24</sup> Even at larger length scales, the mechanically cleaved samples of WSe<sub>2</sub> are atomically flat, as can be seen in the inset of Figure 1. Only a few electronic defects can be observed in an area of 80 × 80 nm<sup>2</sup>. The average terrace size of WSe<sub>2</sub> is very large, and step edges are only rarely encountered in STM scans.

After the deposition of about a quarter of a monolayer of silicon on clean WSe<sub>2</sub>, the WSe<sub>2</sub> surface displays more roughness in the STM topography scans than the bare surface, as can be seen in Figure 2(a). A hill-and-valley structure can be observed in the topography scans, similar to the observations by Chiappe *et al.*<sup>16</sup> and Molle *et al.*<sup>17</sup> for the silicon on MoS<sub>2</sub> system. Upon the deposition of more silicon, the surface becomes even rougher and after a few monolayers eventually 3D clusters are observed on the surface.

It is not obvious at all that the growth does resemble typical island growth, as was suggested by Chiappe *et al.*<sup>16</sup> for the Si/MoS<sub>2</sub> system. A firm argument against island growth is the fact that the lattice constant of the hill-and-valley is exactly the same as the lattice constant of the bare WSe<sub>2</sub> or MoS<sub>2</sub> substrates. This is not compatible with the silicon island growth on top of WSe<sub>2</sub> since the lattice constants of silicon or low-buckled silicene are substantially larger.<sup>25</sup> Chiappe *et al.*<sup>16</sup> interpreted the observed small lattice constant as the growth of strained high-buckled silicene. They argued that high-buckled silicene grows epitaxially on MoS<sub>2</sub>, i.e., the lattice constant of silicene adapts itself to the lattice constant of the MoS<sub>2</sub> substrate. However, it should be pointed out that freestanding high-buckled silicene is unstable because it has imaginary phonon modes in a large portion of the Brillouin zone.<sup>26,27</sup> In

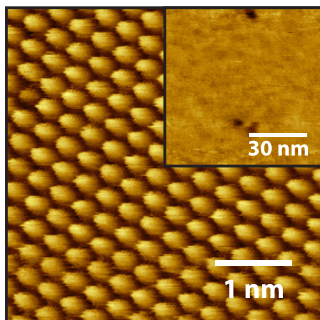


FIG. 1. The clean atomically resolved surface of WSe<sub>2</sub> ( $V = -0.6$  V,  $I = 1.1$  nA). Inset: Large area scan of WSe<sub>2</sub> showing a few electronic defects.

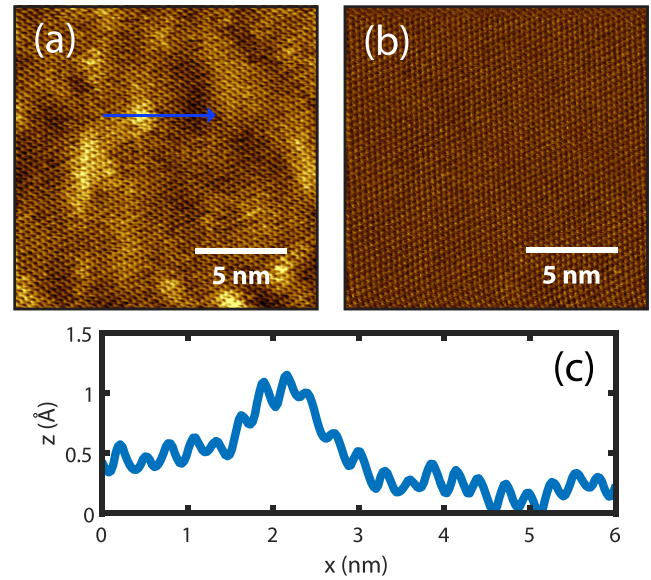


FIG. 2. Constant current topography (a) and  $dI/dz$  (b) maps of WSe<sub>2</sub> after deposition of 0.25 ML of silicon ( $V = -0.8$  V,  $I = 1.5$  nA). The  $dI/dz$  map is proportional to the local apparent barrier height. The maps are recorded simultaneously. The line profile indicated in (a) is displayed in panel (c).

addition, the interaction between the silicon adlayer and the substrate is governed by weak van der Waals forces and therefore the formation of a strained epitaxial silicon layer is highly unlikely. Actually, van der Waals heteroepitaxy has been demonstrated even for materials with a large lattice mismatch.<sup>28</sup>

Another strong argument against island growth is that the transition from a hill to a valley is very gradual, as can be seen in the line profile in Figure 2(c). In the case of island growth on top of a substrate, one expects to encounter well-defined island edges, which show up as abrupt height variations in the constant current STM scans. The gradual transition from a hill to a valley does, however, support the idea of a buckled WSe<sub>2</sub> top layer.

At this point, it is still not clear what the hills and valleys in the topography scans exactly represent. This is because a constant current topography scan in the STM contains both topographic and electronic information. In order to determine the exact nature of the hill-and-valley structure, one needs to separate the topographic and electronic signals and obtain chemical sensitivity on the surface. In STM, this can be accomplished by operating the STM in the  $dI/dz$  spectroscopy mode. The  $dI/dz$  signal can be recorded simultaneously with the constant current topography. In the constant current mode, the z-piezo voltage is measured (the z-piezo voltage can be converted into a height  $z_0$ , which should be discriminated from,  $z$ , the tip-sample distance), whereas in the  $dI/dz$  mode only the derivative of the current to  $z$  is measured. The fact that the  $dI/dz$  signal is not dependent on the local surface height variations can easily be understood within the framework of the Tersoff and Hamann approximation.<sup>29</sup> The tunnel current  $I$  is given by

$$I = C \int_0^{eV} \rho_t(E - eV) \rho_s(E) T(V, E, z) dE, \quad (1)$$

where  $C$  is a proportionality constant,  $e$  the elementary charge,  $V$  the applied voltage between tip and sample and  $\rho_t$  and  $\rho_s$  the density of states of the tip and sample, respectively.  $T(V, E, z)$  is the tunneling probability and  $E$  and  $z$  are the electron energy and the tip-sample distance, respectively. The tunneling probability depends on the tip-sample distance  $z$ , but not  $z_0$

$$T(V, E, z) = \exp\left(-2\frac{\sqrt{2m}}{\hbar}z\sqrt{\varphi_A + \frac{eV}{2} - E}\right), \quad (2)$$

with  $m$  the electron mass and  $\varphi_A$  the local apparent barrier height<sup>30</sup> that is equal to  $(\varphi_s + \varphi_t)/2$ , where  $\varphi_s$  and  $\varphi_t$  are the work functions of the sample and the tip, respectively. The derivative of this tunneling probability is given by

$$\begin{aligned} \frac{dT}{dz} &= T(V, E, z) \left(-2\frac{\sqrt{2m}}{\hbar}\sqrt{\varphi_A + \frac{eV}{2} - E}\right) \\ &= A(V, E)T(V, E, z). \end{aligned} \quad (3)$$

We emphasize that  $A(V, E)$  does not depend on  $z$ . When we insert Equation (2) of  $T(V, E, z)$  in the expression of the current  $I$  in Equation (1),  $dI/dz$  is given by

$$\frac{dI}{dz} = C \int_0^{eV} \rho_t(E - eV)\rho_s(E) \frac{T(V, E, z)}{dz} dE = A(V, E)I. \quad (4)$$

Here,  $dI/dz$  does not depend on  $z_0$ , i.e., the extension of the  $z$ -piezo, or  $z$ , the tip-sample distance. For small sample biases, i.e.,  $eV/2 \ll \varphi_A$ , one finds

$$\frac{1}{I} \frac{dI}{dz} = \frac{d \ln(I)}{dz} \approx \frac{2\sqrt{2m}}{\hbar} \sqrt{\varphi_A}. \quad (5)$$

The apparent barrier height is related to the local sample work function as stated earlier and is sensitive to the chemical composition of the surface. The measured apparent barrier height has experimentally been found to be independent of the tip-sample distance for reasonable tunnel gaps up until the point of contact.<sup>31</sup> During constant current scanning, the height of the tip is constantly adjusted as to keep a constant tunneling current. To record these  $dI/dz$  maps, a small sinusoidal signal (with a frequency that exceeds the bandwidth of the feedback loop) is applied to the  $z$ -piezo during scanning at constant current. The resulting oscillations in the current can be accurately detected by a lock-in technique.

Simultaneously with the topography in Figure 2(a), the  $dI/dz$  map as shown in Figure 2(b) was obtained. As can be seen, the  $dI/dz$  map does not show any contrast besides the atomic corrugation. This atomic corrugation is a result of lateral variations of the decay length of the surface wave functions, as discussed in more detail by Wiesendanger.<sup>30</sup> With the topographic information removed, it is even more clear that there is one continuous lattice. Also, since the topographic information is removed from this scan, we conclude that the electronic properties of the hills and valleys are identical. This would not be the case if the hills were silicon islands because this would result in a contrast variation of the measured apparent barrier height. Therefore, we have to conclude that there is actually no silicon at all on the surface

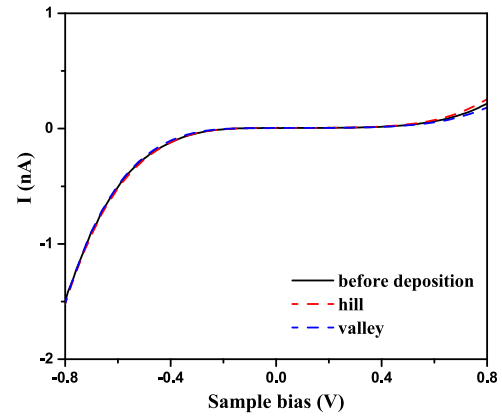


FIG. 3.  $I(V)$  curves recorded on  $\text{WSe}_2$  ( $V = -0.8$  V and  $I = 1.5$  nA) before deposition (black curve), after the deposition of 0.25 monolayers of Si on a hill (red curve) and a valley (blue curve).

of  $\text{WSe}_2$ . The outer-most layer of the hill and valley structure is pure  $\text{WSe}_2$ , and therefore silicon must have been intercalated in between the top layers of  $\text{WSe}_2$ . These results are supported by  $I(V)$  spectra recorded on the bare  $\text{WSe}_2$  surface before and after the deposition of silicon in Figure 3. In order to compare the  $I(V)$  traces of the bare  $\text{WSe}_2$  surface and hills and valleys that are found after deposition, we have taken all  $I(V)$  traces with the same set points ( $V = -0.8$  V and  $I = 1.5$  nA). As can be seen in Figure 3, all three  $I(V)$  curves share the same semiconductor characteristics with similar bandgap.

Finally, it should be noted that intercalation is ubiquitous in TMDs because intercalated atoms can exchange charge more easily than atoms located on top of the TMD.<sup>32</sup> Intercalation has been found to occur through defects or steps in the surface.<sup>33</sup> The diffusion barrier on van der Waals materials is very low, and therefore the adatoms can easily reach step edges or defects, even though the defect density is rather low.<sup>34</sup> Intercalation in TMDs is the rule rather than the exception for small atoms such as sodium and lithium,<sup>33,35</sup> but even large atoms, such as cesium and gold, can intercalate.<sup>36–38</sup>

In summary, the deposition of silicon on  $\text{WSe}_2$  has been studied with scanning tunneling microscopy and spectroscopy. Upon the deposition of silicon, a hill-and-valley structure develops that has a lattice constant that has the exact same value as the TMD substrate. Spatial maps of the  $dI/dz$  provide compelling evidence that silicon does not grow on top of  $\text{WSe}_2$  but rather intercalates between the top layers of  $\text{WSe}_2$ .

Q.Y. thanks the China Scholarship Council for financial support. R.v.B. and H.J.W.Z. thank the Stichting voor Fundamenteel Onderzoek der Materie (FOM, FV157 14TWDO07) for the financial support.

<sup>1</sup>K. S. Novoselov, A. K. Geim, S. V. Morozov, D. Jiang, Y. Zhang, S. V. Dubonos, I. V. Grigorieva, and A. A. Firsov, *Science* **306**, 666 (2004).

<sup>2</sup>H. Rydberg, M. Dion, N. Jacobson, E. Schröder, P. Hyldgaard, S. I. Simak, D. C. Langreth, and B. I. Lundqvist, *Phys. Rev. Lett.* **91**, 126402 (2003).

<sup>3</sup>M. Xu, T. Liang, M. Shi, and H. Chen, *Chem. Rev.* **113**, 3766 (2013).

<sup>4</sup>K. F. Mak, C. Lee, J. Hone, J. Shan, and T. F. Heinz, *Phys. Rev. Lett.* **105**, 136805 (2010).

- <sup>5</sup>H. Li, Q. Zhang, C. C. R. Yap, B. K. Tay, T. H. T. Edwin, A. Olivier, and D. Baillargeat, *Adv. Funct. Mater.* **22**, 1385 (2012).
- <sup>6</sup>R. Balog, B. Jørgensen, L. Nilsson, M. Andersen, E. Rienks, M. Bianchi, M. Fanetti, E. Lægsgaard, A. Baraldi, S. Lizzit, Z. Slijivancanin, F. Besenbacher, B. Hammer, T. G. Pedersen, P. Hofmann, and L. Hornekær, *Nat. Mater.* **9**, 315 (2010).
- <sup>7</sup>J.-S. Park and H. J. Choi, *Phys. Rev. B* **92**, 045402 (2015).
- <sup>8</sup>G. G. Guzmán-Verri and L. C. Lew Yan Voon, *Phys. Rev. B* **76**, 075131 (2007).
- <sup>9</sup>B. Lalmi, H. Oughaddou, H. Enriquez, A. Kara, S. Vizzini, B. Ealet, and B. Aufray, *Appl. Phys. Lett.* **97**, 223109 (2010).
- <sup>10</sup>H. Jamgotchian, Y. Colignon, N. Hamzaoui, B. Ealet, J. Y. Hoarau, B. Aufray, and J. P. Bibérian, *J. Phys. Condens. Matter Inst. Phys. J.* **24**, 172001 (2012).
- <sup>11</sup>P. Vogt, P. De Padova, C. Quaresima, J. Avila, E. Frantzeskakis, M. C. Asensio, A. Resta, B. Ealet, and G. Le Lay, *Phys. Rev. Lett.* **108**, 155501 (2012).
- <sup>12</sup>H. Enriquez, S. Vizzini, A. Kara, B. Lalmi, and H. Oughaddou, *J. Phys.: Condens. Matter* **24**, 314211 (2012).
- <sup>13</sup>M. X. Chen and M. Weinert, *Nano Lett.* **14**, 5189 (2014).
- <sup>14</sup>C.-L. Lin, R. Arafune, K. Kawahara, M. Kanno, N. Tsukahara, E. Minamitani, Y. Kim, M. Kawai, and N. Takagi, *Phys. Rev. Lett.* **110**, 076801 (2013).
- <sup>15</sup>N. Gao, J. C. Li, and Q. Jiang, *Phys. Chem. Chem. Phys.* **16**, 11673 (2014).
- <sup>16</sup>D. Chiappe, E. Scalise, E. Cinquanta, C. Grazianetti, B. van den Broek, M. Fanciulli, M. Houssa, and A. Molle, *Adv. Mater.* **26**, 2096 (2014).
- <sup>17</sup>A. Molle, A. Lamperti, D. Rotta, M. Fanciulli, E. Cinquanta, and C. Grazianetti, *Adv. Mater. Interfaces* **3**, 1500619 (2016).
- <sup>18</sup>L. Li, S. Lu, J. Pan, Z. Qin, Y. Wang, Y. Wang, G. Cao, S. Du, and H.-J. Gao, *Adv. Mater.* **26**, 4820 (2014).
- <sup>19</sup>M. E. Dávila, L. Xian, S. Cahangirov, A. Rubio, and G. L. Lay, *New J. Phys.* **16**, 095002 (2014).
- <sup>20</sup>P. Bampoulis, L. Zhang, A. Safaei, R. van Gastel, B. Poelsema, and H. J. W. Zandvliet, *J. Phys.: Condens. Matter* **26**, 442001 (2014).
- <sup>21</sup>A. Acun, L. Zhang, P. Bampoulis, M. Farmanbar, A. van Houselt, A. N. Rudenko, M. Lingenfelder, G. Brocks, B. Poelsema, M. I. Katsnelson, and H. J. W. Zandvliet, *J. Phys.: Condens. Matter* **27**, 443002 (2015).
- <sup>22</sup>L. Zhang, P. Bampoulis, A. N. Rudenko, Q. Yao, A. van Houselt, B. Poelsema, M. I. Katsnelson, and H. J. W. Zandvliet, *Phys. Rev. Lett.* **116**, 256804 (2016).
- <sup>23</sup>L. Zhang, P. Bampoulis, A. van Houselt, and H. J. W. Zandvliet, *Appl. Phys. Lett.* **107**, 111605 (2015).
- <sup>24</sup>W. J. Schutte, J. L. De Boer, and F. Jellinek, *J. Solid State Chem.* **70**, 207 (1987).
- <sup>25</sup>S. Lebègue and O. Eriksson, *Phys. Rev. B* **79**, 115409 (2009).
- <sup>26</sup>S. Cahangirov, M. Topsakal, E. Aktürk, H. Şahin, and S. Ciraci, *Phys. Rev. Lett.* **102**, 236804 (2009).
- <sup>27</sup>N. J. Roome and J. D. Carey, *ACS Appl. Mater. Interfaces* **6**, 7743 (2014).
- <sup>28</sup>A. Koma, K. Sunouchi, and T. Miyajima, *Microelectron. Eng.* **2**, 129 (1984).
- <sup>29</sup>J. Tersoff and D. R. Hamann, *Phys. Rev. B* **31**, 805 (1985).
- <sup>30</sup>R. Wiesendanger, *Scanning Probe Microscopy and Spectroscopy: Methods and Applications*, 1st ed. (Cambridge University Press, Cambridge England, New York, 1994).
- <sup>31</sup>L. Olesen, M. Brandbyge, M. R. Sorensen, K. W. Jacobsen, E. Laegsgaard, I. Stensgaard, and F. Besenbacher, *Phys. Rev. Lett.* **76**, 1485 (1996).
- <sup>32</sup>M. S. Whittingham and R. R. Chianelli, *J. Chem. Educ.* **57**, 569 (1980).
- <sup>33</sup>F. Xiong, H. Wang, X. Liu, J. Sun, M. Brongersma, E. Pop, and Y. Cui, *Nano Lett.* **15**, 6777 (2015).
- <sup>34</sup>M. Petrović, I. Šrut Rakić, S. Runte, C. Busse, J. T. Sadowski, P. Lazić, I. Pletikosić, Z.-H. Pan, M. Milun, P. Pervan, N. Atodiresei, R. Brako, D. Šokčević, T. Valla, T. Michely, and M. Kralj, *Nat. Commun.* **4**, 2772 (2013).
- <sup>35</sup>H. E. Brauer, H. I. Starnberg, L. J. Holleboom, V. N. Strocov, and H. P. Hughes, *Phys. Rev. B* **58**, 10031 (1998).
- <sup>36</sup>C. Pettenkofer, W. Jaegermann, A. Schellenberger, E. Holub-Krappe, C. A. Papageorgopoulos, M. Kamaratos, and A. Papageorgopoulos, *Solid State Commun.* **84**, 921 (1992).
- <sup>37</sup>H. I. Starnberg, H. E. Brauer, L. J. Holleboom, and H. P. Hughes, *Phys. Rev. Lett.* **70**, 3111 (1993).
- <sup>38</sup>F. Iyikanat, H. Sahin, R. T. Senger, and F. M. Peeters, *APL Mater.* **2**, 092801 (2014).